VIP Cadmium Sulfide Nanoparticles

DOI: 10.1002/anie.201301709

Carbon-Coated CdS Petalous Nanostructures with Enhanced Photostability and Photocatalytic Activity**

Yong Hu, Xuehui Gao, Le Yu, Yanrong Wang, Jiqiang Ning, Shijie Xu, and Xiong Wen (David) Lou**

Cadmium sulfide (CdS), one of the most technologically important semiconductor materials, has applications in a wide range of fields including optoelectronics,[1] photovoltaics,[2] chemical sensors,[3] and photocatalysis.[4] With a bandgap of around 2.4 eV, which matches well with the visible spectral range of solar irradiation, CdS exhibits excellent photocatalytic activity because of its highly effective absorption of solar energy. As a visible-light-driven photocatalyst, it has been extensively investigated and its photocatalytic activity has been found to be influenced by a variety of factors including preparation conditions, particle size, morphology, and crystallinity.[5] For example, features such as good crystallinity, large surface area, and a hexagonal crystal phase have been found to favor higher photocatalytic activity.[6] Although numerous nanostructured CdS materials with various morphologies have been reported, such as nanospheres,[7] nanotubes,[8] nanowires,[9] nanocubes,[10] and nanobelts,[11] it is still challenging to synthesize highly active CdS photocatalysts with controllable size, morphology, and high crystallinity. Moreover, there is an inherent drawback for CdS-based photocatalysts: the photocorrosion problem,[12] in which the sulfide ion is highly prone to oxidation by photogenerated holes. The photocorrosion effect makes CdS very unstable as a photocatalyst and greatly obstructs its practical application. Another great concern of CdS-based photocatalysts is the toxicity of leached Cd^{2+} ions. It is therefore absolutely vital to develop suitable surface engineering methods to inhibit photocorrosive damage to the CdS nanoparticles. Coating CdS with a thin layer of amorphous carbon may be an effective method to stabilize the surface and inhibit the photocorrosion process.[13] Amorphous carbon is an interesting and unique coating material for nanostructures, and it can be obtained by inexpensive and environmentally benign hydrothermal or solvothermal processes, simply using glucose as a precursor.[14] More importantly, the properties of the final product might also be modified, such as optical and catalytic properties, and the absorbtion capacity, by modification of the carbon nanocoating.[15]

Herein, we report a facile route for one-pot solvothermal preparation of CdS petalous nanostructures coated with a thin layer of carbon. The as-prepared nanohybrids have an interesting structure consisting of mostly four petals in a tetrahedral geometry, and the petalous nanoparticles are very uniform in size. Each individual petal unit is cone-shaped and the high surface area is retained after assembly into a multi-petalous geometry. The carbon nanocoating remarkably improves the photostability and the photocatalytic efficiency of the CdS photocatalyst for the degradation of methyl orange (MO) and rhodamine B (RhB). As revealed by optical spectroscopic measurements, the carbon layer not only significantly reduces the amount of surface traps, but also provides perfect chemical protection to inner CdS nanoparticles. As a result of the carbon layer protection, the photocorrosion of CdS is successfully inhibited.

A series of samples were synthesized by adding different amounts of glucose. Specifically, 0, 0.25, 0.5, 0.75 and 1.0 g of glucose were used, and the samples were named as CdS, CdS-C-0.25, CdS-C-0.5, CdS-C-0.75, and CdS-C-1.0, respectively. The crystallographic structure and phase purity of the as-prepared samples were examined by X-ray powder diffraction (XRD). A typical XRD pattern recorded from the sample CdS-C-0.5 is shown in Figure 1. All of the diffraction peaks can be indexed to the hexagonal CdS with lattice constants of $a = 4.140$ Å and $c = 6.719$ Å (JCPDS card no. 41-1049). No cubic phase or impurity peaks can be detected from the XRD measurement. The XRD patterns of all other samples confirm formation of the hexagonal CdS phase (see the Supporting Information, Figure S1). Because of X-ray scattering by the deposited amorphous carbon layer, reduced diffraction intensity is observed.[13]

Scanning electron microscope (SEM) images of the as-prepared CdS-C product (sample CdS-C-0.5) are shown in Figure 2 a,b. These images reveal that the nanoparticles are very uniform, about 300 nm in size, and are made up of four petal-like units. Each petal has a cone-like shape, and the assembly of four petals into this kind of geometry retains the large surface area of these anisotropic petal units. For comparison, SEM images of other samples prepared with

[*] Prof. Y. Hu, X. H. Gao, Y. R. Wang
Key Laboratory of the Ministry of Education for Advanced Catalysis Materials, Institute of Physical Chemistry
Zhejiang Normal University, Jinhua, 321004 (P.R. China)
E-mail: yonghu@zjnu.edu.cn
Dr. J. Q. Ning, Prof. S. J. Xu
Department of Physics and HKU-CAS Joint Laboratory on New Materials, The University of Hong Kong
Pokfulam Road, Hong Kong (P.R. China)
L. Yu, Prof. X. W. Lou
School of Chemical and Biomedical Engineering, Nanyang Technological University, 62 Nanyang Drive
Singapore 637459 (Singapore)
E-mail: xwlou@ntu.edu.sg
Homepage: http://www.ntu.edu.sg/home/xwlou

[**] Financial support from the Natural Science Foundation of China (21171146), Zhejiang Provincial Natural Science Foundation of China (Y4110304) is gratefully acknowledged.

Supporting information for this article is available on the WWW under http://dx.doi.org/10.1002/anie.201301709.

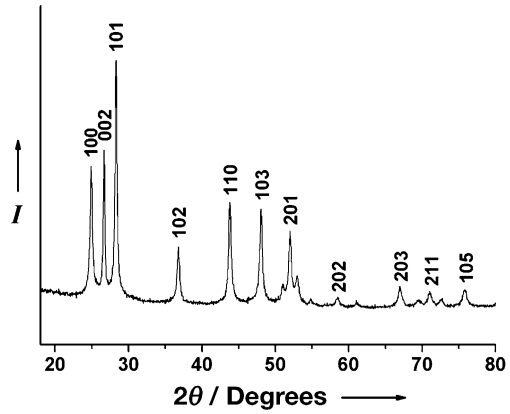

Figure 1. XRD pattern of carbon-coated CdS petalous particles obtained with 0.5 g of glucose.

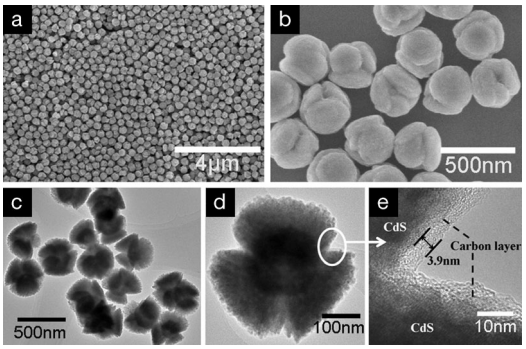

Figure 2. SEM (a,b), TEM, and HRTEM (c–e) images of CdS-C-0.5.

different amounts of glucose are provided in Figure S2, all of which reveal the same petalous morphology. However, the size of the petalous particles slightly reduces as the amount of glucose increases. The morphology and structure of these petalous particles are further elucidated by TEM, as shown in Figure 2c,d. One can see the uniform tetrapetalous nanostructures, which are in good agreement with the SEM observation. Figure 2e displays a high-resolution TEM (HRTEM) image of an individual particle. It can be clearly seen that the crystalline CdS particle is coated with an amorphous carbon layer of about 3.9 nm in thickness. The carbon coating in other CdS-C products that were obtained with different amounts of glucose is also revealed by HRTEM examination (Figure S3). It is clear that the thickness of the amorphous carbon layer depends directly on the amount of glucose added in the synthesis. The carbon layer thickness varies (from 2.5 to 6.0 nm) with the amount of glucose added (0.25–1.0 g). Both the CdS and CdS-C-0.5 samples exhibit relatively small Brunauer-Emmett-Teller (BET) specific surface areas of 3.15 and 6.02 $m^2 g^{-1}$, respectively, with few mesopores (Figure S4).

It should be emphasized here that the use of ethylene glycol (EG) as the solvent and polyvinylpyrrolidone (PVP) as the shape modifier is critical for the formation of dispersed uniform petalous particles. When the synthesis is carried out in either an aqueous solution or EG, but in the absence of PVP, only dendritic particles are formed (Figure S5). These results support the determinative role of EG and PVP in the growth process of CdS petalous particles. It is speculated that the PVP macromolecules are able to arrest the nuclei to form organic–inorganic hybrids in the initial growth progress. The PVP-stabilized hybrids then spontaneously assemble to form the multipetalous geometry.[16–18] The coating of the carbon layer onto the CdS petalous particles is realized by simply introducing a certain amount of glucose into the growth solution. When the reaction temperature is high enough, the glucose starts to polymerize and then carbonize,[19] and finally a layer of amorphous carbon is coated onto the CdS particles.

Confocal micro-Raman spectroscopy was utilized to characterize the functionality of the carbon nanocoating in the CdS-C hybrid particles. An Ar^+ laser was used as the light source for the Raman scattering measurements. The energy of its 514.5 nm light is nearly resonant with the bandgap of CdS materials, and therefore the laser heating effect was expected to be very prominent, owing to intensive absorption at this wavelength. We took advantage of the laser heating effect to examine the photostability of CdS-C hybrid particles. Figure 3

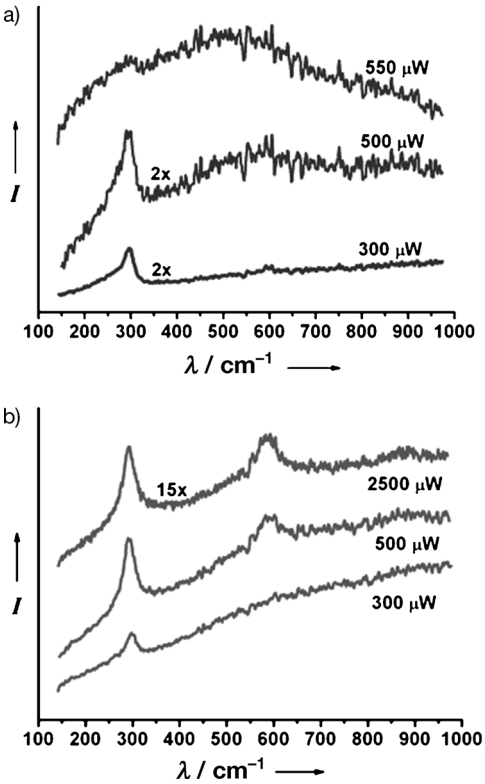

Figure 3. Raman spectra of pure CdS particles (a), and CdS-C-0.5 (b) measured at different laser powers.

shows a typical Raman spectra measured with different laser powers from both pure (Figure 3a) and carbon-coated CdS particles (Figure 3b, CdS-C-0.5). At a power of 300 μW, both samples exhibit a Raman active peak at about 295 cm^{-1}, which is the characteristic LO phonon mode of nanosized CdS materials.[20] When the excitation power increases to 500 μW, the Raman spectra from both samples start to change. The CdS-C-0.5 sample exhibits an overtone of two LO phonons at

about 588 cm^{-1},[21] whereas the pure CdS sample shows a broadened line feature around the two-photon Raman scattering range. When the laser power is slightly increased to 550 μW (Figure 3a), the characteristic Raman peak of CdS disappears from the spectral line measured from the pure CdS sample. On the contrary, for the carbon-coated CdS particles, even at a power of 2500 μW, the Raman peak at 295 cm^{-1} is still observable. Moreover, the relative intensity of the two-phonon overtone at about 588 cm^{-1} gets enhanced with respect to the first-order LO mode, and even the third-order Raman scattering mode at about 883 cm^{-1} becomes detectable. As the intensity ratio of the two-phonon LO mode to the one-phonon LO mode is a measure of the strength of electron–phonon interaction,[22] we attribute the enhanced relative intensity to further crystallization of CdS particles owing to the laser heating effect. From this Raman study, one can see the important protective effect of the carbon layer on the CdS particles. At a laser power of 500 μW, the laser heating effect becomes significant, and remarkable thermal impact can be induced on the CdS particles. In pure CdS particles, laser-heating-induced photocorrosion occurs very easily, resulting in the oxidation of S^{2-} under irradiation at the 514.5 nm laser line. The oxidation of the CdS particles appears so severe that the Raman signal of CdS completely disappears at a laser power of 550 μW, which indicates serious damage to the CdS crystal. It is believed that, as a result of photocorrosion, CdS is oxidized into CdO, which is similar to the oxidation of pure CdS particles annealed at 450 °C in air (Figure S6). In contrast, the carbon-coated CdS particles are resistant to photocorrosion damage, even at a laser power of 2500 μW. Furthermore, with the protection of the carbon nanocoating, the crystallinity of the CdS particles gets improved under laser heating. These results suggest that the carbon layer can effectively serve as a protective coating for the CdS particles.

UV/Vis diffuse reflectance spectroscopy (DRS) was employed to characterize the absorption property of the CdS petalous particles with carbon coating. The DRS results acquired from the samples are presented in Figure 4. All of the spectra exhibit the same absorption band from the shorter wavelength side to around 550 nm, which corresponds to the band-gap absorption of CdS. Distinct absorption behaviors occur at the sub-bandgap absorption range. Compared with the pure CdS particles, all of the carbon-coated samples show enhanced visible-light absorption. When the carbon layer becomes much thicker, the absorbance drops, especially at longer wavelengths. This observation reveals that a thick carbon layer results in increased diffuse reflectivity and deteriorates the light absorption ability of the hybrid particles. Therefore, control over the carbon layer thickness is crucial to visible light absorption by carbon-coated CdS particles. Moreover, photoluminescence (PL) spectroscopy measurements (Figure S7) further indicate that the carbon coating on the CdS particles effectively passivates the CdS surface. Therefore, one can see the multifunctional role of the carbon nanocoating in the CdS-C hybrid particles, including passivating the surface of the CdS nanospheres, enhancing visible light absorption, and protecting the CdS core from photocorrosion. All of these effects are expected to enhance the photocatalytic performance of this interesting hybrid nanostructure.

The photocatalytic activity of the CdS-C hybrid particles was evaluated for the degradation of organic dyes, MO and RhB, under visible-light irradiation. Figure 5a presents the visible-light photocatalytic degradation of MO in the presence of different photocatalysts. Compared with pure CdS particles, all of the carbon-coated CdS samples exhibit enhanced photocatalytic efficiency. After irradiation for 40 min, the degradation fractions for different photocatalysts

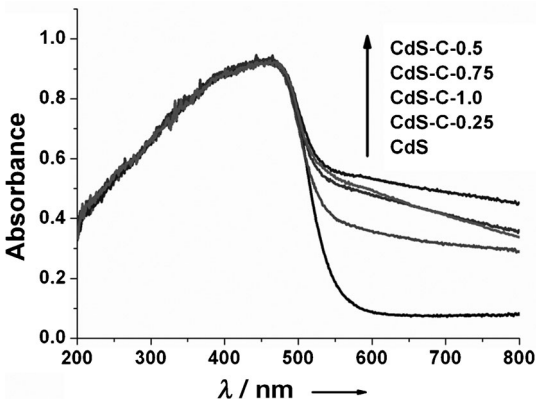

Figure 4. Diffuse reflectance UV/Vis spectra of pure CdS and CdS-C hybrid particles.

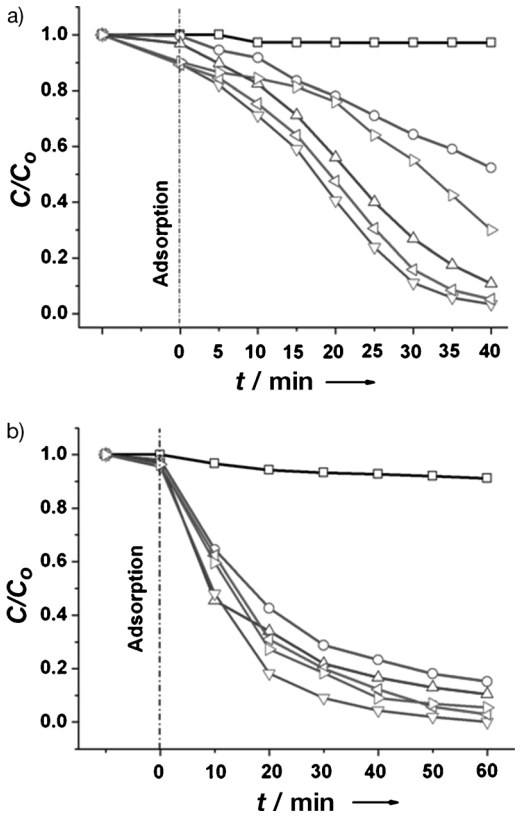

Figure 5. The photodegradation of MO (a), and RhB (b) in the presence of different photocatalysts under visible-light irradiation. Blank (□; included for comparison), CdS (○), CdS-C-0.25 (△), CdS-C-0.5 (▽), CdS-C-0.75 (◁), CdS-C-1.0 (▷).

are 47.8% (pure-CdS), 89.3% (CdS-C-0.25), 96.6% (CdS-C-0.5), 94.8% (CdS-C-0.75), and 70.0% (CdS-C-1.0). Figure 5b displays the photocatalytic degradation results of RhB in the presence of different photocatalysts. As with the degradation of MO, the CdS-C-0.5 sample again exhibits the highest photocatalytic activity among all of the samples. The improvement in the degradation of RhB brought on by carbon nanocoating is less pronounced than in the degradation of MO; this is probably due to the larger size of the RhB molecules, which makes them more difficult to penetrate the carbon layer. The above results reveal that the carbon nanocoating on the CdS particles remarkably improves the photocatalytic efficiency. Specifically, the amorphous carbon layer can enhance the adsorption capability for organic dyes, which can enrich the dye molecules on the surface of photoactive CdS particles, thus resulting in the acceleration of photocatalytic reactions. However, a thick and dense carbon layer may reduce the inherent optical absorption of CdS and result in a rapid decrease in photogenerated charges, ultimately reducing the photocatalytic activity.[23] Thus, there should be an optimal thickness of the amorphous carbon layer. We have further studied the stability and reusability of the CdS-C-0.5 photocatalyst by collecting and reusing the photocatalyst for four cycles (Figure S8). The results show that there is only an insignificant loss in the photocatalytic activity, which might be partly caused by loss of the photocatalyst during each round of collection and rinsing. The XRD pattern and SEM image of the photocatalyst after four cycles of photodegradation testing also demonstrate the intact structure and morphology (Figure S9). Lastly, we also performed measurements of ·OH radicals on CdS-C hybrid and pure CdS particles using a previously reported method (Figure S10).[24] It was observed that the photogenerated holes are powerful enough to oxidize surface-adsorbed hydroxy groups and water molecules to generate ·OH radicals. Also, the maximum amount of ·OH radicals is formed in the photoreaction process mediated by the CdS-C-0.5 photocatalyst, which is in good agreement with the above results for the photodegradation of MO and RhB.

In summary, we have developed a facile one-pot solvothermal method to synthesize carbon-coated CdS petalous nanostructures with uniform morphology. The carbon nanocoating has been found to have multiple functions, including protection of the CdS surface, enhancement of visible light absorption, and facilitating the separation of photogenerated charges. The resulting CdS-C hybrid particles exhibit excellent photostability and enhanced photocatalytic activity for the degradation of MO and RhB. The synergistic effect between CdS and the carbon nanocoating was also investigated through the measurement of ·OH radicals produced by CdS-C hybrid photocatalysts with different carbon layer thicknesses. It is believed that this synthesis method can be extended to prepare a wide variety of functional nanohybrids for different applications.

Received: February 27, 2013
Published online: April 8, 2013

Keywords: cadmium · nanoparticles · photochemistry

[1] X. L. Li, Y. Jia, A. Y. Cao, *ACS Nano* **2010**, *4*, 506.
[2] Z. X. Pan, H. Zhang, K. Cheng, Y. M. Hou, J. L. Hua, X. H. Zhong, *ACS Nano* **2012**, *6*, 3982.
[3] A. Ferancová, S. Rengaraj, Y. Kim, J. Labuda, M. Sillanpää, *Biosens. Bioelectron.* **2010**, *26*, 314.
[4] a) Y. Hu, Y. Liu, H. S. Qian, Z. Q. Li, J. F. Chen, *Langmuir* **2010**, *26*, 18570; b) Y. Liu, L. Zhou, Y. Hu, C. F. Guo, H. S. Qian, F. M. Zhang, X. W. Lou, *J. Mater. Chem.* **2011**, *21*, 18359; c) W. L. Yang, Y. Liu, Y. Hu, M. J. Zhou, H. S. Qian, *J. Mater. Chem.* **2012**, *22*, 13895.
[5] X. B. Chen, S. H. Shen, L. J. Guo, S. S. Mao, *Chem. Rev.* **2010**, *110*, 6503.
[6] N. Z. Bao, L. M. Shen, T. Takata, K. Domen, A. Gupta, K. Yanagisawa, C. A. Grimes, *J. Phys. Chem. C* **2007**, *111*, 17527.
[7] C. L. Li, J. Yuan, B. Y. Han, W. F. Shangguan, *Int. J. Hydrogen Energy* **2011**, *36*, 4271.
[8] C. Z. Wang, Y. F. E, L. Z. Fan, Z. H. Wang, H. B. Liu, Y. L. Li, S. H. Yang, Y. L. Li, *Adv. Mater.* **2007**, *19*, 3677.
[9] N. Z. Bao, L. M. Shen, T. Takata, D. L. Lu, K. Domen, *Chem. Lett.* **2006**, *35*, 318.
[10] C. C. Chen, J. J. Lin, *Adv. Mater.* **2001**, *13*, 136.
[11] L. Li, P. C. Wu, X. S. Fang, T. Y. Zhai, L. Dai, M. Y. Liao, Y. Koide, H. Q. Wang, Y. Bando, D. Golberg, *Adv. Mater.* **2010**, *22*, 3161.
[12] a) D. N. Ke, S. L. Liu, K. Dai, J. P. Zhou, L. N. Zhang, T. Y. Peng, *J. Phys. Chem. C* **2009**, *113*, 16021; b) A. Kudo, Y. Miseki, *Chem. Soc. Rev.* **2009**, *38*, 253.
[13] Y. Guo, H. S. Wang, C. L. He, L. J. Qiu, X. B. Cao, *Langmuir* **2009**, *25*, 4678.
[14] a) H. W. Liang, W. J. Zhang, Y. N. Ma, X. Cao, Q. F. Guan, W. P. Xu, S. H. Yu, *ACS Nano* **2011**, *5*, 8148; b) B. Hu, K. Wang, L. H. Wu, S. H. Yu, M. Antonietti, M. M. Titirici, *Adv. Mater.* **2010**, *22*, 813; c) G. X. Wang, H. Liu, J. Liu, S. Z. Qiao, G. Q. M. Lu, P. Munroe, H. Ahn, *Adv. Mater.* **2010**, *22*, 4944.
[15] M. J. Zhou, Y. Hu, Y. Liu, W. L. Yang, H. S. Qian, *CrystEngComm* **2012**, *14*, 7686.
[16] L. Fan, R. Guo, *Cryst. Growth Des.* **2009**, *9*, 1677.
[17] H. Cölfen, S. Mann, *Angew. Chem.* **2003**, *115*, 2452; *Angew. Chem. Int. Ed.* **2003**, *42*, 2350.
[18] a) A. P. Alivisatos, *Science* **2000**, *289*, 736; b) Z. Tang, N. A. Kotov, M. Giersig, *Science* **2002**, *297*, 237; c) A. Narayanaswamy, H. F. Xu, N. Pradhan, M. Kim, X. G. Peng, *J. Am. Chem. Soc.* **2006**, *128*, 10310; d) A. Narayanaswamy, H. F. Xu, N. Pradhan, X. G. Peng, *Angew. Chem.* **2006**, *118*, 5487; *Angew. Chem. Int. Ed.* **2006**, *45*, 5361.
[19] X. M. Sun, Y. D. Li, *Angew. Chem.* **2004**, *116*, 607; *Angew. Chem. Int. Ed.* **2004**, *43*, 597.
[20] R. Kostić, N. Romčević, *Phys. Status Solidi C* **2004**, 2646.
[21] M. Abdulkhadar, B. Thomas, *Nanostruct. Mater.* **1995**, *5*, 289.
[22] J. J. Shiang, S. H. Risbud, A. P. Alivisatos, *J. Chem. Phys.* **1993**, *98*, 8432.
[23] Y. Y. Li, J. P. Liu, X. T. Huang, J. G. Yu, *Dalton Trans.* **2010**, *39*, 3420.
[24] a) W. L. Yang, L. Zhang, Y. Hu, Y. J. Zhong, H. B. Wu, X. W. Lou, *Angew. Chem.* **2012**, *124*, 11669; *Angew. Chem. Int. Ed.* **2012**, *51*, 11501; b) J. H. Huang, K. N. Ding, X. C. Wang, X. Z. Fu, *Langmuir* **2009**, *25*, 8313; c) G. Liu, P. Niu, L. C. Yin, H. M. Cheng, *J. Am. Chem. Soc.* **2012**, *134*, 9070.

